Valence band structure of $TlSbS_2$ crystals by angle-resolved photoemission

1992 J. Phys.: Condens. Matter 4 887

(http://iopscience.iop.org/0953-8984/4/3/028)

J. Phys.: Condens. Matter 4 (1992) 887–894. Printed in the UK

Valence band structure of $TlSbS_2$ crystals by angle-resolved photoemission

G Lévêque†, J Olivier-Fourcade‡ and J C Jumas‡

† Laboratoire d'Etudes des Surfaces, Interfaces et Composants, Université de Montpellier II, Sciences et Techniques du Languedoc, place Eugène Bataillon, 34095 Montpellier Cédex 5, France

‡ Laboratoire de Physicochimie des Matériaux Solides, Université de Montpellier II, Sciences et Techniques du Languedoc, place Eugène Bataillon, 34095 Montpellier Cédex 5, France

Received 4 February 1991, in final form 17 September 1991

Abstract. Photoemission is performed on $TlSbS_2$, a layered compound with a large unit cell (16 atoms) and a calculated structure of 28 valence bands. The angle-integrated emission data confirm the existence of three groups of bands as obtained in the tight-binding calculation.

In the angle-resolved mode, the observed emission presents a large energy dispersion with an apparent period larger than the reciprocal lattice. This effect, also present in other materials having a large number of atoms by unit cell, is attributed to strong variations versus $k_{\parallel}$ of the transition matrix elements.

In this case, photoemission data are not directly comparable with the band structure and a complete calculation of emission probability is needed to assign the observed bands.

1. Introduction

Lone-pair elements, such as antimony(III), lead to the formation of various atomic arrangements in the chalcogenide family [1]. In these complex structures the local atomic arrangement around Sb can be described as a distorted incomplete octahedron (with one, two or three missing apexes) with their optoelectronic characteristics varied within a large range.

A general study has been undertaken [2] using several experimental techniques (x-ray diffraction, x-ray absorption, Mössbauer spectroscopy, XPS and UPS) and band-structure calculations [3, 4] to determine the links between the atomic structure and their electronic properties.

We report here the photoemission spectra of $TlSbS_2$, a compound which belongs to a largely unexplored class of chain ternary crystals [5, 6]. This compound crystallizes in a triclinic distorted NaCl structure [7]. In the $TlSb_2$–Sb_2S_3 binary system, four definite compounds have been synthesized [8]: Tl_3SbS_3, $TlSbS_2$, $TlSb_3S_5$ and $TlSb_5S_8$, all of them composed of chains of Sb–S bonds or Tl–S bonds (figure 1). Tight-binding calculations [4] performed on several of these compounds emphasize the role of the non-bonding state in the coordination of Sb atoms and in the formation of the chains.

The optical and electrical properties of the semiconductor $TlSbS_2$ have already been studied [9–11]. The present work was intended to verify the band structures reported in

0953-8984/92/0300887 + 08 $03.50

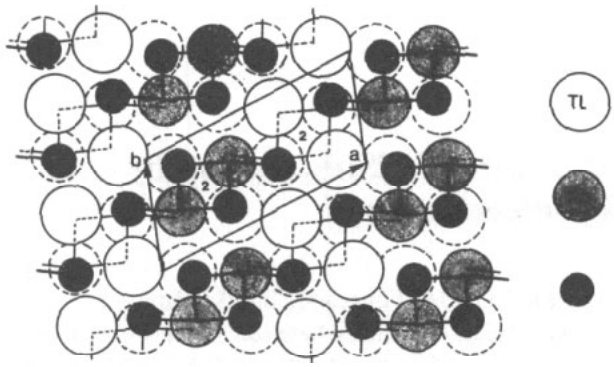

Figure 1. Top view of the basal surface of the crystal $TlSbS_2$. The first layer of atom is represented by bold lines. The inversion centre is at the centre of the unit cell. The size of the atoms are taken according to the atomic radii used in band-structure calculations [4]. The shorter Sb–S bonds are plotted in order to enhance the Sb–S chains of atoms.

[4] and eventually to test the basic assumption made in the LCAO model. The main difficulty we expected comes from the significant number of atoms (16) in one unit cell, giving 28 non-degenerated sp valence bands in an energy interval of approximately 6 eV. With such numerous bands, and the present energy resolution of our device of 0.2 eV, most individual bands cannot be split as mentioned in equivalent photoemission studies [12–14]. We expect here to observe only prominent features of the valence band structure.

2. Experiment

Single crystals of $TlSbS_2$ were grown by the classical Bridgman method [8] and are cleaved by pealing *in situ* in vacuum (10^{-9} Torr) just before the photoemission experiments. Like other layered materials, cleaved $TlSbS_2$ has a limited chemical reactivity and the samples are free of detectable contamination during the experiments.

The photoemission experiments were performed with an apparatus already described [15] and shown in figure 2. All electrons emitted in the plane defined by azimuthal angle ψ are dispersed by a toroidal magnetic field and focused onto a fluorescent screen. The position on the screen of the electron impacts are determined by the dispersive optics and allows direct determination of the kinetic energy E_{kin} and polar angle θ.

The electron initial state $(E_i, k_\parallel)$ can be deduced easily according to the usual relations

$$k_\parallel = (2m/\hbar^2)^{1/2} E_{kin}^{1/2} \sin\theta \tag{1}$$

$$E_i = E_{kin} - h\nu + \varphi. \tag{2}$$

As the above relations are monotonic, the display of the electron impacts on the screen gives a real-time direct visualization of the valence band structure $E_i(k_\parallel)$ with only

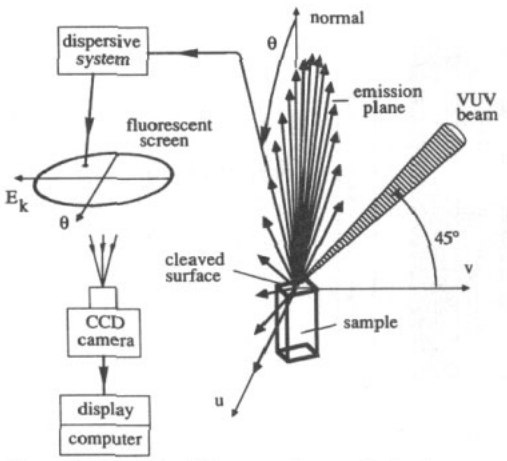

Figure 2. Principle of the experiment. Each electron emitted in the plane selected by the device is dispersed and focused onto the detector (microchannel plates + fluorescent screen): VUV, vacuum ultraviolet. It gives a visible point with the kinetic energy E_{kin} as the abscissa and the polar angle θ as the ordinate. Different azimuthal angles ψ are obtained by rotating the sample around the normal. The VUV beam is unpolarized.

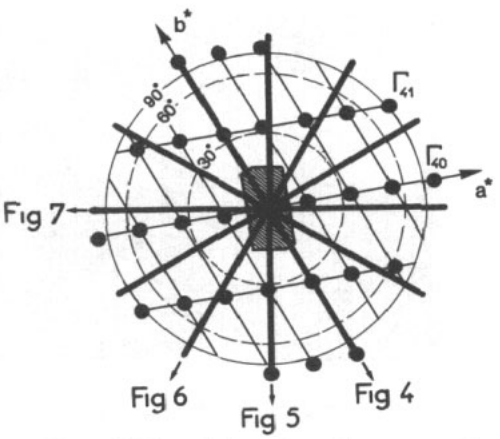

Figure 3. Zone of the reciprocal space tested in photoemission, for polar angles 30°, 60° and 90° and a kinetic energy of 16 eV. The labels a^* and b^* indicate the directions of the a^* and b^* vectors which form the lattice represented by light lines. The full circles represent the Γ_{mn} points. The bold lines mark the six different planes of photoemission studied here. The two-dimensional Brillouin zone is represented at the centre of the figure.

a slight distortion. The different azimuthal directions ψ of the Brillouin zone are probed by rotating the sample around the normal. Six different ψ-values (30° spaced) have been studied in order to test the significant part of the two-dimensional reciprocal space.

The images of emission distributions given by the electron impacts on the screen are recorded numerically and processed to remove the optic distortion and the vertical black lines (which are shadows of the dispersive system). The images are further processed to improve band aspect and contrast (see figures 4(*b*), 5(*b*), 6(*b*) and 7(*b*)).

We show in figure 3 the position of the six studied planes relative to the developed reciprocal lattice. According to the small size of the Brillouin zone, most of the experimental $k_{\parallel}$-values correspond to high-order zones. We then used the periodic lattice representation. The symbol Γ_{mn} refers to the lattice node $ma^* + nb^*$. Only the data in planes 1, 2, 3 and 5 are presented with their closest band structures in figures 4–7.

3. Discussion

Figures 4–7 compare the experimental photoemission intensity with the calculated band structure [4]. The calculations are performed in a tight-binding approximation scheme, using the mean interaction coefficient of Harrisson [16] and Allan and Lannoo [17] limited to a small number of neighbours: for the first neighbour at distance R_1,

$$H_{\alpha\beta}(R_1) = -(\hbar^2/m)(n_{\alpha\beta}/R_1^2) \tag{3}$$

and, for other atoms between R_1 and $R_c \simeq 3.2$ Å,

$$H_{\alpha\beta}(d) = H_{\alpha\beta}(R_1)\exp[-2.5(d/R_1 - 1)].$$

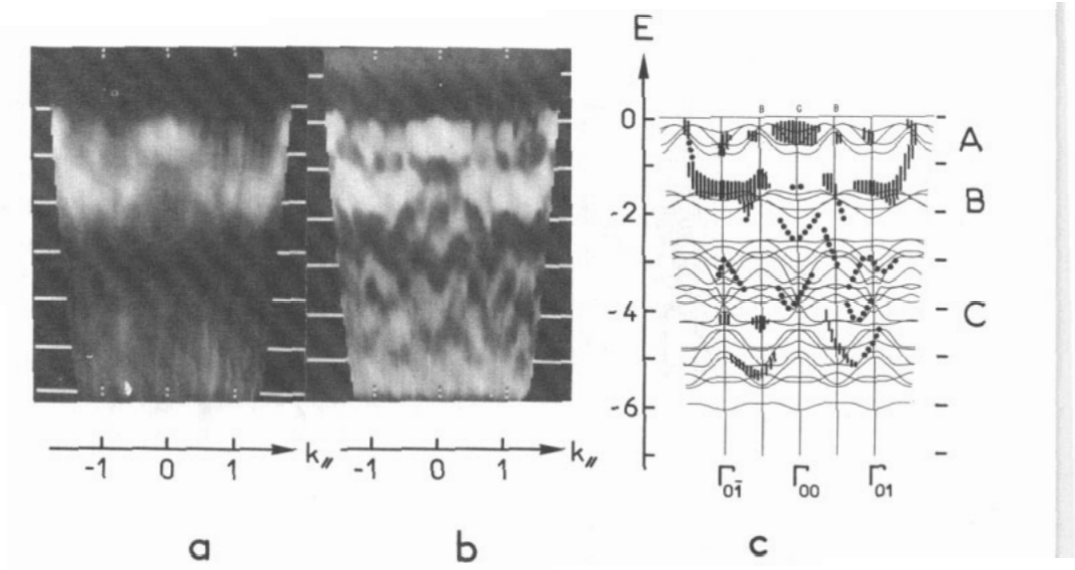

Figure 4. Emission intensity in the $E,k_{\parallel}$ plane for $h\nu = 21.2$ eV (unpolarized). (*a*) Results from our experiment, for direction 1 in figure 3 ($\psi = 0°$). (*b*) Result of image processing which enhances the bands (and also some of the noise). Two energy scales are used: in (*a*), the conventional binding energy is relative to the photoemission threshold and, in (*b*), a translated energy scale is used whose origin is at the first band and compares more easily with the band calculation. (*c*) Band structure from [4]. Experimental data are reported as full circle for narrow bands and a shaded area for diffuse emission. The energies are in electronvolts, and $k_{\parallel}$ in reciprocal ångströms.

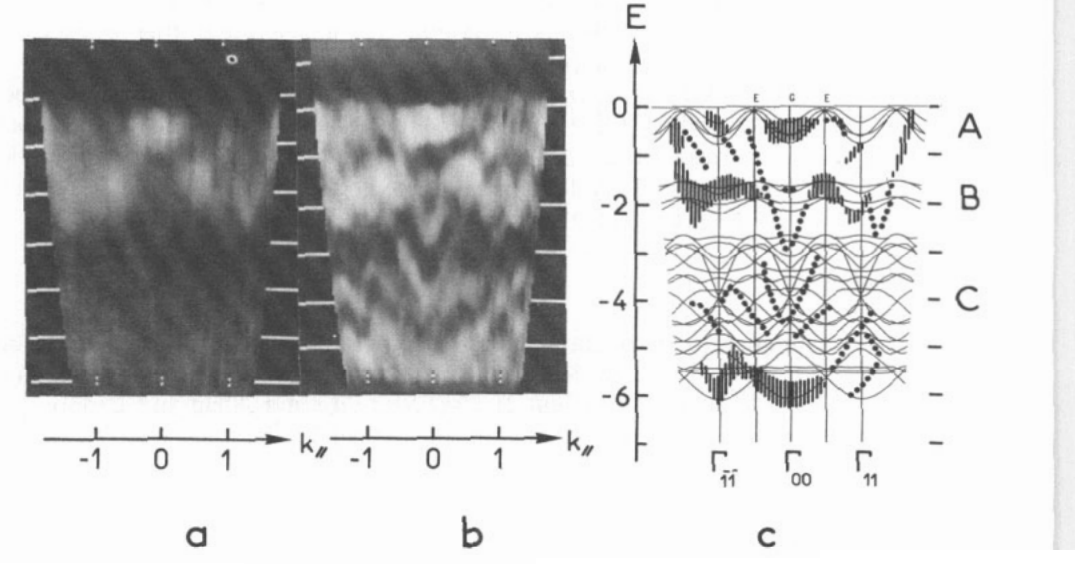

Figure 5. Same as figure 4 for direction 2 ($\psi = 30°$).

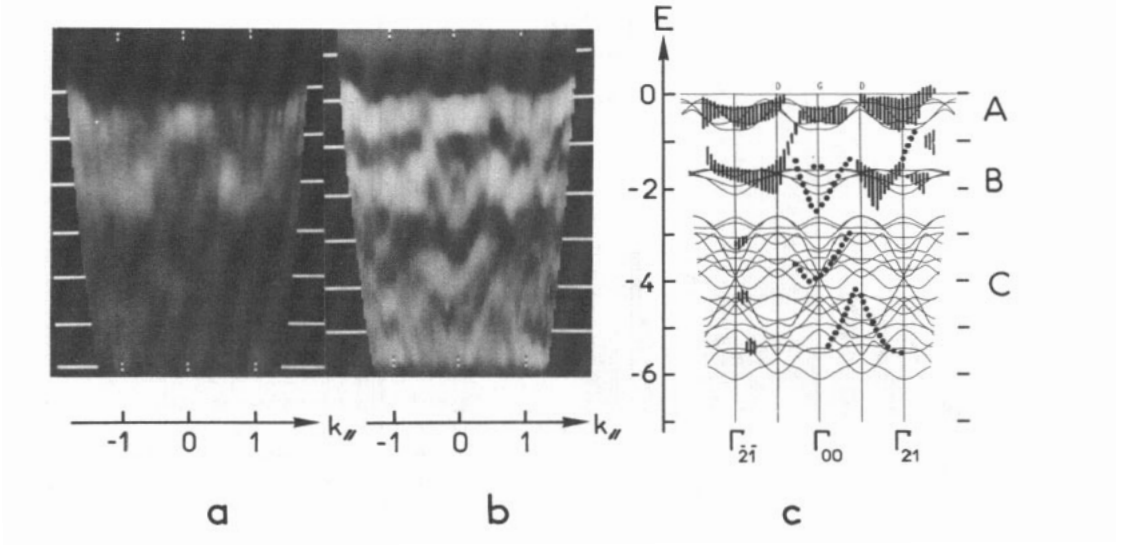

Figure 6. Same as figure 4 for direction 3 ($\psi = 60°$).

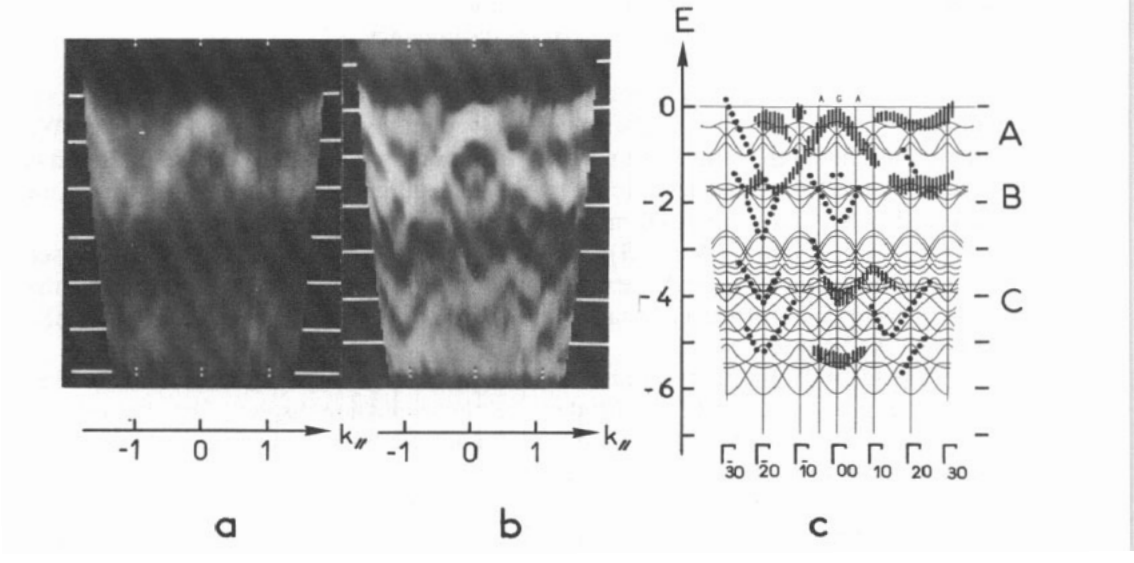

Figure 7. Same as figure 4 for direction 5 ($\psi = 120°$).

The calculated 28 valence bands can be divided into three non-overlapping groups: group A, four bands mainly s(Tl) + p(S); group B, four bands mainly s(Tl) + s(Sb) + p(S); group C, 20 bands mainly p(S) + p(Sb).

The comparison between the photoemission data and the calculated bands is at first disappointing as one observes a complex pattern with few individual bands. The top of the valence band appears on the different images as a large diffuse structure. Moreover,

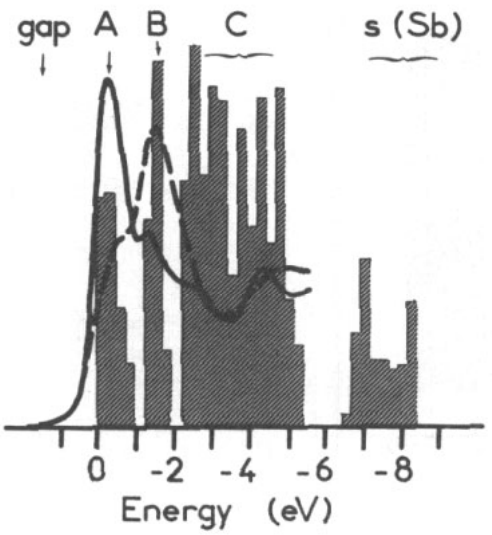

Figure 8. Comparison between different data on the valence band of $TlSbS_2$: ▨, histogram of density of states from the tight-binding calculation [4]; ———, EDC for $\theta = 0$ (normal emission); – – –, EDC for $\theta = 20°$, averaged over all ψ-values.

the $k_\parallel$ dispersion of the emission intensity seems to obey a different period from the reciprocal lattice (see top of figure 3 for example).

We shall examine carefully this apparent discrepancy.

(1) In figure 8, we give selected photoemission energy distribution curves (EDCs), obtained by averaging some of the angle-resolved intensities shown in figures 4–7. We note on these EDCs that the three peaks correspond approximately to the A, B and C groups of bands from the calculation. Owing to the different emission cross sections for s and p orbitals, our results confirm the separation of the bands into three groups.

The two upper bands (A and B) are also clearly seen in the angle-resolved data (see figure 6). The bands in group A are maximum for normal emission ($k_\parallel = 0$), whereas the bands of group B are stronger around $k_\parallel \simeq \pm 1$ Å^{-1}. The third group C is diffuse at the bottom of the image.

(2) The second point to be discussed is the apparent discrepancy between the period of the reciprocal lattice and the period of the photoemission display. This discrepancy may come from the neglect of $k_\perp$ dispersion in our analysis. To understand this point, one must recall the particular structure of the layered compound $TlSbS_2$ and the mean distances calculated between the atoms [7]: Sb–S, 2.60 Å along the chains; Sb–S, 3.70 Å between the chains; Sb–S, 4.91 Å between the layers. These distances are to be compared with the critical distance $R_c = 3.09$ Å used in the band calculation, and the van der Waals distance $R_{vDW} = 3.85$ Å.

For Tl–S bands we note the following: Tl–S, 3.15 Å along the chains; Tl–S, 3.20 Å between the chains; Tl–S, 3.51 Å between the layers. The corresponding values are $R_c = 3.41$ Å and $R_{vDW} = 3.76$ Å.

This R_c-value indicates that the band calculation does not take into account any bonds between layers. The result is a true two-dimensional calculated band structure with no dispersion along $k_\perp$. As the Tl–S distance is of the order of the van der Waals bond length, a weak bonding exists between the layers, giving a dispersion of the group of bands A and B along $k_\perp$ for the real structure.

Applying equation (3) to Tl–S bonding between layers gives a non-negligible matrix element of the order of 0.8 eV. This three-dimensional effect of the band structure is of a magnitude sufficient to explain the modulation in emission intensity versus θ, but we cannot conclude this before a more complete band calculation is achieved.

(3) We neglect the possible reconstruction of the surface. This is done for two reasons. Firstly, as weak bonds are opened by cleavage, the surface of the sample is not too far from energetic equilibrium and the reconstruction may not be needed. Secondly, the reconstructions usually produce a surface unit cell larger than the projection of the volume unit cell, which is the opposite of the observed phenomenon.

(4) The last acceptable explanation for the observed period discrepancy is an unusually strong variation in the emission matrix elements along $k_\parallel$. As already noticed in the case of crystals with a complex crystallographic structure [12–14] or with additional surface symmetry [18–21], large variations in the transition matrix elements with $k_\parallel$ may occur, eventually masking the valence band dispersion.

4. Conclusion

It appears that our photoemission data are compatible with available band-structure calculations, but a direct comparison between the two sets of data is not yet possible because of the small size of the Brillouin zone which allows for a strong effect of $k_\perp$ dispersion and large matrix element variations.

The apparent period in the $k_\parallel$-space seems to be $4a^*$ and $a^*–b^*$, corresponding to a 'virtual' unit cell in the real space, four times smaller than the real one, and containing only one molecule of $TlSbS_2$. The variation in the matrix element may then be correlated to interference effects between the four different molecules of the real unit cell, but a complete calculation of the photoemission intensities from the matrix elements is needed to analyse further and to understand our experimental data.

Acknowledgments

We are very grateful to Professor M Lannoo and I Lefebvre for providing us with the unpublished band structures in a form adapted to our project.

References

[1] Ibanez A, Olivier-Fourcade J, Jumas J C, Philippot E and Maurin M 1986 *Z. Anorg. (Allg.) Chem.* **540–541** 106

[2] Olivier-Fourcade J, Ibanez A, Jumas J C, Maurin M, Lefebvre I, Lippens P, Lannoo M and Allan G 1990 *J. Solid State Chem.* **87** 366

[3] Lefebvre I, Lannoo M, Allan G, Ibanez A, Olivier-Fourcade J, Jumas J C and Beaurepaire E 1987 *Phys. Rev. Lett.* **59** 2471

[4] Lefebvre I 1989 *Doctorat Sciences des Matériaux* Lille

[5] Rouxel J 1986 *Crystal Chemistry and Properties of Materials with Quasi One Dimensional Structure* (Dordrecht: Reidel) p 1

[6] Margaritondo G 1986 *Physics and Chemistry of Material with Low Dimensional Structure* ed V Grasso (Dordrecht: Reidel) p 399

[7] Rey N, Jumas J C, Olivier-Fourcade J and Philippot E 1983 *Acta Crystallogr.* C **39** 971

[8] Jumas J C, Olivier-Fourcade J, Rey N and Philippot E 1985 *Rev. Chimie Minéral.* **22** 651

[9] Rouquette P, Allègre J, Mathieu H, Ance C and Olivier-Fourcade J 1986 *Solid State Commun.* **59** 899
[10] Rouquette P, Camassel J, Bastide G, Martin L, Olivier-Fourcade J and Philippot E 1986 *Solid State Commun.* **60** 709
[11] Rouquette P, Allègre J, Gil B, Camassel J, Mathieu H, Ibanez A and Jumas J C 1986 *Phys. Rev.* B **33** 4114
[12] Kilday D C, Niles D W, Margaritondo G and Levy F 1987 *Phys. Rev.* B **35** 660
[13] Mirami F, Kimura J and Takekawa S 1989 *Phys. Rev.* B **39** 4788
[14] Takahashi T, Matsuyama H, Katayama H, Okabe Y, Hosoya S, Seki S, Fujimoto H, Sako M and Inokuchi H 1989 *Phys. Rev.* B **39** 6636
[15] Leveque G and Robin J 1987 *Rev. Sci. Instrum.* **58** 1456
[16] Harrisson W A 1981 *Phys. Rev.* B **24** 5835
[17] Allan G and Lannoo M 1983 *J. Physique* **44** 1355
[18] Holland B W and Woodruff D P 1973 *Surf. Sci.* **36** 488
[19] Precia D, Law A R, Jonhson M T and Hughes H P 1983 *Solid State Commun.* **56** 809
[20] Prince K C, Surman M, Lindner T and Badshaw A M 1986 *Solid State Commun.* **59** 71
[21] Prince K C 1987 *J. Electron Spectrosc.* **42** 217